Mechanical and Energy Engineering

Energy and Exergy Analysis of Dual Channel Solar Air Collector with Different Absorber Plates Geometry

Najim A. Jassim
Assistant Professor
Engineering College-University of Baghdad
najmosawe@gmail.com

Suhaib J. Shbailat
M.Sc Candidate
Engineering College-University of Baghdad
suhaib@ieee.org

ABSTRACT

Flat-plate collector considers most common types of collectors, for ease of manufacturing and low price compared with other collectors. The main aim of the present work is to increase the efficiency of the collector, which can be achieved by improving the heat transfer and minimize heat loss experimentally. Five types of solar air collectors have been tested, which conventional channel with a smooth absorber plate (model I), dual channel with a smooth absorber plate (model II), dual channel with perforating "V" corrugated absorber plate (model III), dual channel with internal attached wire mesh (model IV), and dual channel with absorber sheet of transparent honeycomb, (model V). The dual channel collector used for increasing heat transfer area and heat removal factor to improve thermal performance. The outdoor test was conducted during the period December (2016) to February (2017) at different mass flow rates 0.0217 kg/s, 0.0271 kg/s and 0.0325 kg/s. The experiments were carried out from 8:30 AM to 3:00 PM for clear days. Experimental results show that the average thermal efficiency was (72.2 %) for model (III), (40.2 %) for model (I), (51.6 %) for model (II), (65.1 %) for model (IV) and (59.7 %) for model (V). At the last part of the study, the exergy analyses were derived for both collectors. The results of this part showed that the conventional channel model (I) is having largest irreversibility, and the dual channel collector model (III) is having a greatest exergetic efficiency.

Keywords: solar air collector; dual channel; double flow; exergy analysis; heat removal factor.

<div dir="rtl">

التحليل الحراري وتحليل الطاقة المتاحة لمجمع شمسي مزدوج القناة يعمل بالهواء باستعمال وسط ماص للحرارة

صهيب جواد كاظم
ماجستير هندسة ميكانيكية
كلية الهندسة – جامعة بغداد

نجم عبد جاسم
استاذ مساعد
كلية الهندسة – جامعة بغداد

الخلاصة

يعتبر المجمع الشمسي المسطح اكثر ألانواع شيوعا ، لسهولة التصنيع والسعر المنخفض مقارنة مع المجمعات الشمسية ألاخرى. الهدف الرئيسي من هذا العمل هو زيادة كفاءة المجمع الشمسي، والتي يمكن تحقيقها من خلال تحسين نقل الحرارة وتقليل فقدان الحرارة تجريبيا. تم تصميم وبناء خمسة أنواع من أجهزة تجميع الهواء الشمسي وهي كالاتي قناة التقليدية مع لوحة امتصاص مسطحة (نموذج I)، قناة مزدوجة مع لوحة امتصاص مسطحة (نموذج II)، قناة مزدوجة مع لوحة امتصاص مموجة "V" ومثقبة (نموذج III)، قناة مزدوجة مع لوحة امتصاص وشبكة معدنية (نموذج VI)، وقناة مزدوجة مع لوح امتصاص نافذ بشكل خلية نحل (نموذج V). أجري الاختبار التجريبي خلال الفترة من ديسمبر (2016) إلى فبراير (2017). أجريت التجارب من الساعة 8:30 صباحا حتى الساعة 3:00 مساء لأيام صافية ولثلاث قيم مختلفه لمعدلات تدفق الهواء (0.0217, 0.0271, 0.0325). بينت النتائج التجريبية ان الكفاءة الحرارية (72.2 %) في النموذج (III), (40.2 %) في

</div>

النموذج)I(, (51.6 %) في النموذج)II(, (65.1 %) في النموذج)VI(, (59.7 %) في النموذج)V(.في الجزء الأخير من الدراسة، تم اجراء تحليل الطاقة المتاحة للمجمعات الشمسية. وأظهرت النتائج أن نموذج القناة التقليدية يحظى بأكبر قدر من الخسائر اللاارجاعية، وأن نموذج القناة المزدوجة يتمتع بأكبر قدر من كفاءة الطاقة المتاحة.

الكلمات الرئيسية: مجمع هواء شمسي, قناة مزدوجة, تدفق مزدوج, الطاقة المتاحة (اكسيرجي), معامل الانتزاع الحراري.

1. INTRODUCTION

The fast exhaustion of fossil fuel resources has required an insistent searching for renewable sources of energy to achieve the growing demand for energy for the future needs and for subsequent generations. As can be seen, the reserves and resource base of fossil fuels are limited and exhaustible. Therefore, It is needful to take into consideration that renewable energy sources as a device of power generation.

Solar energy is the largest popular resource for nonconventional energy. It quantitatively plentiful and available, unfailing for most workable applications, and has no polluting effect on the environment when transformed into useful forms and used. However, its availability is interrupted, that means it is available only during the day. The solar energy used in the air heating process for use in heating and drying processes of agricultural crops to minimize the use of electrical energy and thus rely partly on solar power as aide energy.

Iraq has an excellent geographic location, is one of the relatively hot areas and are available in which solar energy in large quantities throughout the seasons of the year. Research has shown that the rate of sunrise in Iraq up to about 3600 hours per year **Hashim** and **Al-shareda, 1984.**

A solar collector is a simplest and most widely device used to convert the energy in sunlight or solar radiation into a form more usable and storage. It has been designed to collect heat by absorbing the sun's radiation. In solar collector, energy is transfer from the radiant energy of sun source to the fluid by absorbing media, **Garg, 1987.**

Exergy can be defined as the maximum useful work possible to obtain it when the system tends to full thermodynamic equilibrium with the full thermodynamic environment when the system is in contact with all of this environment. Also, exergy could represent the maximum useful work carrying out by the system during the process of tends non-equilibrium system to a state of thermodynamic equilibrium with the thermal reservoir, **Yunus, 2006.**

Recently, modern publications in the scope of solar thermal energy tend to adopt Exergy as a basis to conduct analytical studies. Exergy could represent the maximum possible useful work carrying out by the system of solar collector during the air heating process. An exergy is a useful tool for measuring the performance of energy transformation processes. Consequently, exergy analysis applies to various thermal solar systems.

Ozturk and **Demirel, 2004**, investigated heat transfer characteristics of a packed bed solar air collector. The packed bed of solar air collector was stuffed with gravel cylindrical rings which called Raschig rings for storing solar energy. The results showed that the packing improves the heat transfer and the energetic and exergetic efficiencies of the solar air collector with the packed bed are improved 33.78% and 2.16% respectively.

Ozturk, 2005, investigated experimentally of solar air collectors with heat storage unit. A paraffin wax as a PCM was used in a solar collector for heating of the greenhouse and it was contacted each other in a parallel method. Energy and exergy analyses were applied in order to

evaluate the system efficiency. The results showed that the energy efficiency of the greenhouse is improved about 40.4% and the exergy efficiency is improved about 4.2%.

Ucar and **Inalli, 2006,** investigated the shape and arrangement absorber plate of the solar air collector. The surface of absorber plate arranged to increase heat transfer which in turn increased the efficiency of the collector. The five types of arrangement of absorber plate shape were used. The results showed that the energetic and exergetic efficiencies of the solar air collector with this modifications are improved approximately from 10% to 30% in comparison with the conventional solar collector

Esen, 2008, investigated experimentally solar air collector with several obstacles and without obstacles. The air was flowing upper and under absorber plate and the several types of obstacles were attached to top and bottom of absorber plate. The exergy analysis was presented and derived the exergy relations. The results showed that the energetic and exergetic efficiencies of the solar air collector with the obstacles are improved in comparison with the conventional solar collector as 45% and 38% respectively. Also, It showed that the conventional channel is having largest irreversibility.

Bhandari and **Singh, 2012,** developed a theoretical model to study the performance of different types of flat plate solar air collector. A computer program (MATLAB) was used to give the analysis of temperature distribution in the solar air collector. The three types of flat plate collectors used for this study are a conventional collector, double glazing- single pass collector and double flow air solar collector with interior fins. The different parameters were studied to analysis effect it on the solar air collector such as mass flow rate, the intensity of solar radiation and inlet temperature. The results showed the air solar heater (double flow) has highest thermal efficiency compared with the conventional and double glazing collector at the same mass flow rate.

Bahrehmanda and **Ameri, 2015,** investigated theoretically and experimentally a flat plate solar collector with several covers of glass. They have studied the effect of placing several glass covers on the surface of the solar collector and calculated the thermal loss coefficient from the top of the surface of the solar collector. The results showed that the thermal loss was reduced and the energetic and exergetic efficiencies were improved which mean the efficiency is 53.6% in comparison with single glass cover.

Ravi and **Saini, 2016,** investigated of solar air collector with a double pass and artificial roughness attached on both surfaces of an absorber plate. Artificial roughness was used to expose the absorber plate to the maximum amount of thermal energy and thus pass this heat to the air passing over and under the absorber plate. This requires an increase in the capability of pumping air (high-pressure drop), the work of this (artificial roughness) on the surface of the absorber plates affecting the thermohydraulic factors and the activity of the absorber plate and thermohydraulic performance as used for comparison of air solar heaters with the conventional absorber plate. In this study, two types of artificial roughness were tested as many V-shape discrete and stagger ribs. Different parameters were studied, Reynold numbers (Re) range 2000 to 20000 and relatively stagger ribs value (r/e) range 1 to 2.5. The results showed that the heat transfer and efficiency were improved in comparison with the conventional solar collector. Also, it founded the artificial roughness caused friction loss and pressure drop in the solar air collector.

Shbailat and **Jassim, 2017,** investigated experimentally solar air collector with a dual channel which the air flows both in upper channel and lower channel of the absorber plate for increasing heat transfer area. The exergy analysis was presented and derived the exergy relations. The results showed that the dual channel collector is higher than the conventional collector with increased 11% in thermal efficiency. Also, it showed the conventional channel is having largest irreversibility and the dual channel collector is having a greatest exergetic efficiency.

In this study, reviews techniques of passive heat transfer which used the various elements of artificial roughness, in order to contribute in improving the performance of the air solar heater that done during the last few decades. Most of the review works studied flat plate collector with V-Corrugated and with different sections of fins and obstacles. The work presented in this paper aims to analyze the performance of two kinds of flow channels of collectors, that is a dual channel of flowing air as well as a conventional channel and investigate a new geometry of absorber plates which include the perforating "V" corrugated absorber plate and absorber sheet of transparent honeycomb. At the last, the exergy analysis is studying for different absorber plates geometry.

2. EXPERIMENTAL WORK

The solar collector system was placed in the College of Engineering-University of Baghdad, Baghdad, Iraq, where the solar collector was facing to the south and situated at latitude 33.3° N, longitude 44.4° E. The tilt angle increases in the winter (latitude + 10) degrees because of the low level of the sun to making the incidence solar radiation be vertical on the surface of the solar collector**, Degirmencioglu, 2006.** Wherefore, the collector was south oriented with a tilt angle of 43°. The outdoor test was conducted during the period December (2016) to February (2017). The experiments were carried out from 8:30 AM to 3:00 PM for clear days. **Fig.1** shows the photographic view of the experimental setup.

The work presented in this thesis, it includes design and tests solar air collector to meet the regulations on methods of testing defined in ASHRAE Standard 1986 for determining the thermal performance of solar air collector. This study deals with five different types of solar air collectors **Fig.2, 3.** It has been designed and constructed namely:

- o Model I: Conventional channel with a smooth absorber plate.
- o Model II: Dual channel with a smooth absorber plate.
- o Model III: Dual channel with perforating "V" corrugated absorber plate.
- o Model IV: Dual channel with internal attached wire mesh.
- o Model V: Dual channel with absorber sheet of transparent honeycomb.

The collector dimensions are 900 mm in length, 700 mm in width and 160 mm in the depth which it represents the test section of solar air collector. The conic is constructed on both ends to reducing pressure drop. Also, three vanes have constructed in the inlet of the collector for uniform distribution of flowing air. The inlet and outlet are placed as a circular duct of diameter with 75 mm. It is insulated with 50 mm of fiberglass on the back and side walls. The fan is mounted in the lower part of the solar collector, as shown in the **Fig.4.**

3. THERMAL ANALYSIS

The performance of solar air collector evolved by the energy balance. It is determining the distribution of solar energy incident relative to the energy used, useful about it, and various losses.

The incident solar energy is:

$$Q_i = I_i \cdot A_c \tag{1}$$

Loss of heat occurs from all parts of the solar collector. Although the greatest part of the loss occurs from the absorbent part, the loss from the bottom and sides has a significant effect, the amount of energy lost is calculated from the following equation:

$$Q_l = U_l A_c (T_p - T_a) \tag{2}$$

Where:

U_l = Overall heat transfer coefficient (W/m^2 . K)

A_c = Area of collector surface (m^2)

T_p = Temperature of absorber plate (K)

T_a = Ambient temperature.

Useful heat gain by the solar collector is found in the following equation, **Struckmann, 2008.**

$$Q_u = Q_i - Q_l = I_i(\alpha_p \tau_g) \cdot A_c - U_l A_c (T_p - T_a) \tag{3}$$

Also, the amount of useful energy can be obtained on the base of passing fluid through the collector and carried the amount of heat, as the following equation:

$$Q_u = \dot{m} c_p (T_o - T_i) \tag{4}$$

Heat removal factor has represented the value of effective useful energy to the maximum possible of useful energy. The maximum possible of useful energy occurs when the temperature of absorber plate was at the temperature of inlet fluid, can be expressed as, **Struckmann, 2008.**

$$F_R = \frac{\dot{m} c_p (T_o - T_i)}{A_c[I(\alpha_p \tau_g) - U_l(T_i - T_a)]} \tag{5}$$

therefore, the effective useful energy can be explicated by multiplying the maximum possible of useful energy by the heat removal factor of the collector:

$$Q_u = F_R A_c[I(\alpha_p \tau_g) - U_l(T_i - T_a)] \tag{6}$$

The performance of solar air collector is evolved by the energy efficiency. The potential of solar collector was measured by a concept of energy efficiency in the energy conversion process. Also, it is given an indication about heat absorbed by the collector. It represents by a ratio of actual useful energy to incident solar energy on collector area, as follows.

$$\eta = \frac{Q_u}{I_i \cdot A_c} \tag{7}$$

Thence;

$$\eta = \frac{F_R A_c[I(\alpha_p \tau_g) - U_l(T_i - T_a)]}{I_i \cdot A_c} \tag{8}$$

4. EXERGY ANALYSIS

Entropy was generated due to the friction of flowing air in the solar collector, **Bejan, et al., 1981.** Also, the entropy was transported through the temperature change or thermal heat transfer of the fluid flow. Esen's approach was used to exergy analysis, **Esen, 2007.** considering following assumptions:

- The flow is steady.
- Effects of kinetic and potential energies were ignored.
- Consideration specific heat was constant and ideal gas for air.
- The air humidity was ignored.

The exergy balance of solar air collector that determines the distribution of thermal exergy as follow:

The mass flow rates balance equation can be explicated in the rate formula as:

$$\Sigma \dot{m}_{in} = \Sigma \dot{m}_{out} \tag{9}$$

where $\dot{m}$ is the mass flow rates.

The exergy and energy balances can be expressed when neglected the effect of the changes of kinetic and potential energy in follows rate form, **Ucar,** and **Inalli, 2006.**:

The sum of energies at the entrance the system equals the sum of the energies exiting the system (first law of thermodynamics).

$$\Sigma \dot{E}_{in} = \Sigma \dot{E}_{out} \tag{10}$$

$$\Sigma \dot{E}X_{in} - \Sigma \dot{E}X_{out} - \dot{E}X_{work} = \Sigma \dot{E}X_{dest} \tag{11}$$

Or

$$\dot{E}X_{heat} - \dot{E}X_{work} + \dot{E}X_{mass,in} - \dot{E}X_{mass,out} = \dot{E}X_{dest} \tag{12}$$

Also, the exergy balance can be formulated using Eq. (12), the rate form of as follows rate form.

$$\Sigma \left(1 - \frac{T_e}{T_s}\right) Q_s - \dot{W} + p_o \cdot (dv/dt) + \Sigma \dot{m}_{in}\, \psi_{in} - \Sigma \dot{m}_{out}\, \psi_{out} = \dot{E}X_{dest} \tag{13}$$

Where

Q_s is incident solar energy on the collector surface.

T_e is environment temperature, T_s is the apparent black body temperature of the sun (= 6000 K) **Bejan, et al., 1981.**

$\dot{W}$ is the mechanical power supplied by or to the system (neglected).

$$\psi_{in} = (h_{in} - h_e) - T_e (s_{in} - s_e) \tag{14}$$

$$\psi_{out} = (h_{out} - h_e) - T_e (s_{out} - s_e) \tag{15}$$

where

ψ is specific exergy

Substitute Eqs. (14) and (15) into Eq. (13), it yielded as:

$$\left(1 - \frac{T_e}{T_s}\right) Q_s - \dot{m} \left[(h_{out} - h_{in}) - T_e (s_{out} - s_{in})\right] = \dot{E}X_{dest} \tag{16}$$

The entropy and enthalpy changes are expressed for the air in the collector by, **Ucar** and **Inalli, 2006.**:

$$\Delta s = s_{out} - s_{in} = c_p \ln\frac{T_{f,out}}{T_{f,in}} - R \ln\frac{P_{out}}{P_{in}} \tag{17}$$

$$\Delta h = h_{out} - h_{in} = c_p (T_{f,out} - T_{f,in}) \tag{18}$$

The irreversibility $\dot{E}x_{dest}$ can be can be expressed as the following relation:

$$\dot{E}x_{dest} = T_e\ S_{gen.} \tag{19}$$

$$S_{gen.} = \Delta s + \frac{Q_s}{T_s} \tag{20}$$

Or

$$\dot{E}x_{dest} = \dot{E}x_{in} - \dot{E}x_{out} \qquad\qquad \textbf{Bejan, et al., 1981} \tag{21}$$

The second law efficiency is calculated as:

$$\eta_{II} = 1 - \frac{T_e\ S_{gen}}{[1-(T_e/T_s)]\ Q_s} \tag{22}$$

The following mean temperature was used to determine the physical properties of air:

$$\Delta T_m = (T_{in} + T_{out})/2 \tag{23}$$

5. RESULTS AND DISCUSSIONS

The outdoor test was conducted during the period December (2016) to February (2017). The experiments were carried out from 8:30 AM to 3:00 PM for clear days. This section presents a set up a conventional channel of smooth flat plate collector as a reference for comparison with the other types sequentially **Fig.5** and **Fig.8** and shows the effect of using three different values of mass flow rate.

The basic of the experimental test in this work depends on comparing the five models of solar air collectors at the same weather conditions because the change of solar radiation and ambient temperature effect on the efficiency directly, but it is difficult to set up five collectors together due to its need a large space and high cost. Also, it is difficult to achieve the same weather conditions and clear days because the Iraq climate condition is volatile through three months of tests in the winter as **Table 1**.

Therefore, the experimental tests represent a set up a conventional channel of smooth flat plate collector as a reference for comparison with the other types sequentially, and comparing the percentage of increase in thermal efficiency for solar air collector models relatively as **Table 2**. For this reason, each figure represents two models of solar collectors at same climate conditions and not possible draw all models of solar collectors in the same figure due to different the weather conditions as **Table 1**.

Fig. 9a, 9b, 9c and **9d** show the variation of inlet and outlet air temperature of the five models of solar air collectors with day hours on (20th Dec. 2016 and 12th Jan., 23rd Jan., 5th Feb. 2017). These figures show that the maximum outlet air temperature for two collector models sequentially was (28.4°C) in model (I) and (31.2°C) in model (II) on (20th Dec. 2016), (32.7°C) in model (I) and (39.7°C) in model (III) on (12th Jan. 2017), (32.1°C) in model (I) and (38.2°C) in model (IV) on (23rd Jan. 2017), (32.4°C) in model (I) and (36.7°C) in model (V) on (5th Feb. 2017) experimentally. Model (III) having the highest outlet temperature because the turbulences which created due corrugated ribs of absorber plate geometry and the holes (perforations) in absorber plate, that leads to allow the largest amount of heat transfer from the absorber plate to the flowing air and increase the temperature of outlet air.

Fig. 10a, 10b, 10c and **10d** show the variation of heat removal factor of the five models of solar air collectors with day hours on (20th Dec. 2016 and 12th Jan., 23rd Jan., 5th Feb. 2017). These figures show that the average of heat removal factor for two collector models sequentially was

(0.52) in model (I) and (0.68) in model (II) on (20th Dec. 2016), (0.51) in model (I) and (0.93) in model (III) on (12th Jan. 2017), (0.51) in model (I) and (0.81) in model (IV) on (23rd Jan. 2017), (0.52) in model (I) and (0.74) in model (V) on (5th Feb. 2017) experimentally. The highest value of average heat removal factor happened in the model (III), that represents the value of effective useful energy to the maximum possible of useful energy. Also, that gives the indication about the effectiveness of heat exchange in this geometry of absorber plate.

The variation of the pressure drop through collector for five models of solar collectors experimentally was shown in **Fig.11**. These curves represent the increase in the pressure drop through collector with Reynolds number at clear climate, where the pressure drop through collector increases steadily with Reynolds number and reaches its peak value (96.2 Pa) in model (III) at the highest Reynolds number (29208.4) at mass flow rate (0.0325 kg/s) due high obstruction of air passage through collector. The minimum value of the pressure drop through collector was (19.6 Pa) on the model (I) at the smallest value of Re (19472.3) at a mass flow rate (0.0217 kg/s) due to smooth of absorber plate.

The average thermal efficiency at a long day shown in **Table 2** was (40.2 %) in model (I) and (51.6 %) in model (II) on (20th Dec. 2016), (40.6 %) in model (I) and (72.2 %) in model (III) on (12th Jan. 2017), (41.7 %) in model (I) and (65.1 %) in model (IV) on (23rd Jan. 2017), (42.1 %) in model (I) and (59.7 %) in model (V) on (5th Feb. 2017) experimentally. **Fig. 12** shows the variation of thermal efficiency with mass flow rates (0.0217, 0.0271, 0.0325 kg/s). The results show the efficiency of the collector increases at the mass flow rates of the air inlet the solar collectors are increased and these results are scientifically agreed upon.

The change of the exergy destruction with day hours for five models of solar collectors experimentally was shown in **Fig. 13a, 13b, 13c** and **13d**. The maximum of the exergy destruction at midday was (416.6 W) in model (I) and (404.5 W) in model (II) on (20th Dec. 2016), (438.5 W) in model (I) and (328.7 W) in model (III) on (12th Jan. 2017), (433.9 W) in model (I) and (337.8 W) in model (IV) on (23rd Jan. 2017), (421.3 W) in model (I) and (353.6 W) in model (V) on (5th Feb. 2017). The highest value of exergy destruction in the model (I) due to high thermal losses from absorber plate to ambient.

Fig. 14 shows the variation of exergy destruction with mass flow rate (0.0217, 0.0271, 0.0325 kg/s). The results show the exergy destruction of the collector increases at the mass flow rate of the air inlet the solar collectors is increased.

The variation of the exergy efficiency with day hours for five models of solar collectors experimentally was shown in **Fig.15a, 15b, 15c,** and **15d**. The maximum of the exergy efficiency was (64.1 %) in the model (III) and the minimum was (38.9 %) in the model (I).

Fig. 16 shows the variation of exergy efficiency with mass flow rates (0.0217, 0.0271, 0.0325 kg/s). The results show the exergy efficiency of the collector increases at the mass flow rate of the air inlet the solar collectors is increased.

6. CONCLUSIONS

The conclusions below can be summarized from the experimental investigation of the five models of solar air collectors:

1) The dual channel type of solar air collector model (II) used for increasing heat transfer area and heat removal factor that is leading to improved thermal performance and exergetic efficiency. The average thermal efficiency of solar air collectors was increased by (28.3 %) in the model (II), (77.8 %) in the model (III), (56.1 %) in the model (IV) and (41.8 %) in model (V) comparison with the model (I). The best model which gives higher thermal efficiency was (72.2 %) experimentally in the model (III) (perforating "V" corrugated absorber plate) and the other models ((51.6 %) in model (II), (65.1 %) in model (IV) and (59.7 %) in model (V)).

2) The heat removal factor in model (III) of solar air collector was (0.93) and higher than the another models ((0.52) in model (I), (0.68) in model (II), (0.81) in model (IV) and (0.74) in model (V)). Also, the maximum pressure drop was (96.2 Pa) in the model (III) of solar air collector and minimum pressure drop was (19.6 Pa) in the model (I) of solar air collector.

3) The conventional channel model (I) is having largest exergy destruction (421.3 W), and the dual channel collector model (III) is having lower exergy destruction (328.7 W). The maximum of the exergy efficiency was (64.1 %) in the model (III) and the minimum was (38.9 %) in the model (I).

REFERENCES

- Bejan, Kearney, D. W., and F. Kreith, 1981, *Second law analysis and synthesis of solar collector systems,* Journal of Solar Energy Engineering 103: 23.

- Bahrehmand D., M. Ameri, 2015, *Energy and exergy analysis of different solar air collector systems with natural convection,* Renewable Energy 74- 357e368.

- Bhandari, D., and Dr S. Singh. 2012 "Performance analysis of flat plate solar air collectors with and without fins." International Journal of Engineering Research & Technology (IJERT) 1.6: 5.

- Degirmencioglu, Can. 2006, *The use of cell polyurethane foams in air-type solar collectors as the heat absorbing element*, MS thesis. İzmir Institute of Technology, 2006.

- Duffie, John A., and William A. Beckman, 2013, *Solar engineering of thermal processes.* John Wiley & Sons,

- Esen, Hikmet, 2008, *Experimental energy and exergy analysis of a double-flow solar air heater having different obstacles on absorber plates,* Building and Environment 43.6: 1046-1054.

- Garg, H. P. 1987,. *Advances in Solar Energy Technology*: Volume 3 Heating, Agricultural and Photovoltaic Applications of Solar Energy. Springer Science & Business Media,

- Hashem Bisher, Ibrahim Al-Sharida, 1984, *Principles of Solar Energy*, Kuwait Foundation for the Advancement of Sciences, Printing and Publishing House, 2ed.

- Ozturk HH, Demirel Y. 2004, *Exergy-based performance analysis of packed-bed solar air heaters*, International Journal of Energy Research;28(5):423–32.

- Ozturk HH. 2005, *Experimental evaluation of energy and exergy efficiency of a seasonal latent heat storage system for greenhouse heating*, Energy Conversion and Management; 46(9–10):1523–42.
- Ravi, Ravi Kant, and R. P. Saini. 2016, *"Experimental investigation on performance of a double pass artificial roughened solar air heater duct having roughness elements of the combination of discrete multi V shaped and staggered ribs."* Energy 116: 507-516.
- Shbailat, Suhaib. J., and Jassim, N., 2017, May, *Energy and exergy analysis of a flat plate solar collector with dual channel for air flows*, In 1st International conference on recent trends of engineering sciences and sustainability (COEIA 2017), IEEE.
- Struckmann, Fabio. (2008), *Analysis of a flat-plate solar collector*, Heat and Mass Transport, Project Report, 2008MVK160.
- Ucar, A., and M. Inallı, 2006, *Thermal and exergy analysis of solar air collectors with passive augmentation techniques,* International communications in heat and mass transfer 33.10: 1281-1290.
- Yunus, A. Cengel, and A. Boles Michael, 2006, *Thermodynamics: An engineering approach,* McGraw-Hill, New York

NOMENCLATURE

A_c collector area, (m^2)
C_P specific heat, (kJ/kg K)
D_h hydraulic diameter, (m)
$\dot{E}$ energy rate, (kW)
$\dot{E}x$ exergy rate, (kW)
h heat transfer coefficient, $(W/m^2.K)$
I_i incident solar radiation on the collector surface, (W/m^2)
k thermal conductivity, (W/m. K)
L length of collector, (m)
$\dot{m}$ mass flow rate, (kg/s)
P pressure, (N/m²)
Q energy, (W)
s entropy, (kJ/kg K)
T temperature, (˚C)
U overall heat transfer coefficient, $(W/m^2 \, ˚C)$
$\dot{W}$ work rate or power, (kW)

Subscripts

a   ambient
e   environment
g   glass
i,in   inlet,incident
des.   destruction
m   mean

o,out   outlet
p   plate
s   source
u   useful
gen.   generation
Greek letters
α   absorptance
η   thermal efficiency
$η_{II}$ exergetic efficiency
τ   glass transmittance
ψ   specific exergy

Table 1. Reading schedule for five models of solar air collectors**.**

Type	Date	Flow (kg/s)
Dual channel with conventional channel	20/12/2016	0.0217
	21/12/2016	0.0271
	28/12/2016	0.0325
Model (III) with conventional channel	12/1/2017	0.0217
	16/1/2017	0.0271
	18/1/2017	0.0325
Model (IV) with conventional channel	23/1/2017	0.0217
	24/1/2017	0.0271
	29/1/2017	0.0325
Model (V) with conventional channel	5/2/2017	0.0217
	7/2/2017	0.0271
	13/2/2017	0.0325

Table 2. Percentage of increase in thermal efficiency for solar air collector models

Model	Efficiency	Efficiency for model (I)	Percentage of increase
(II)	51.6	40.2	28.3 %
(III)	72.2	40.6	77.8 %
(IV)	65.1	41.7	56.1 %
(V)	59.7	42.1	41.8 %

Figure 1. Photographic view of experimental setup solar collector.

Model (I) and (II)
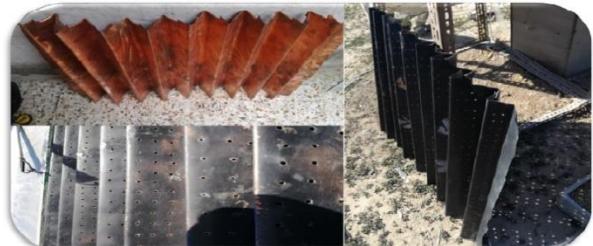
Model (III)

Model (IV)
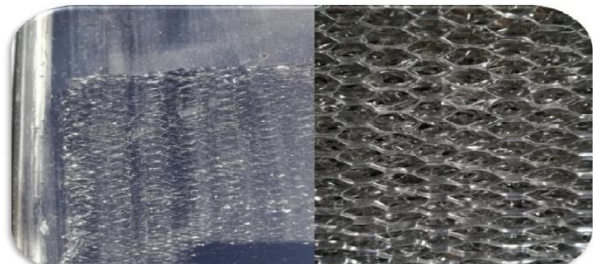
Model (V)

Figure 2. Photographic view for models of absorber plates.
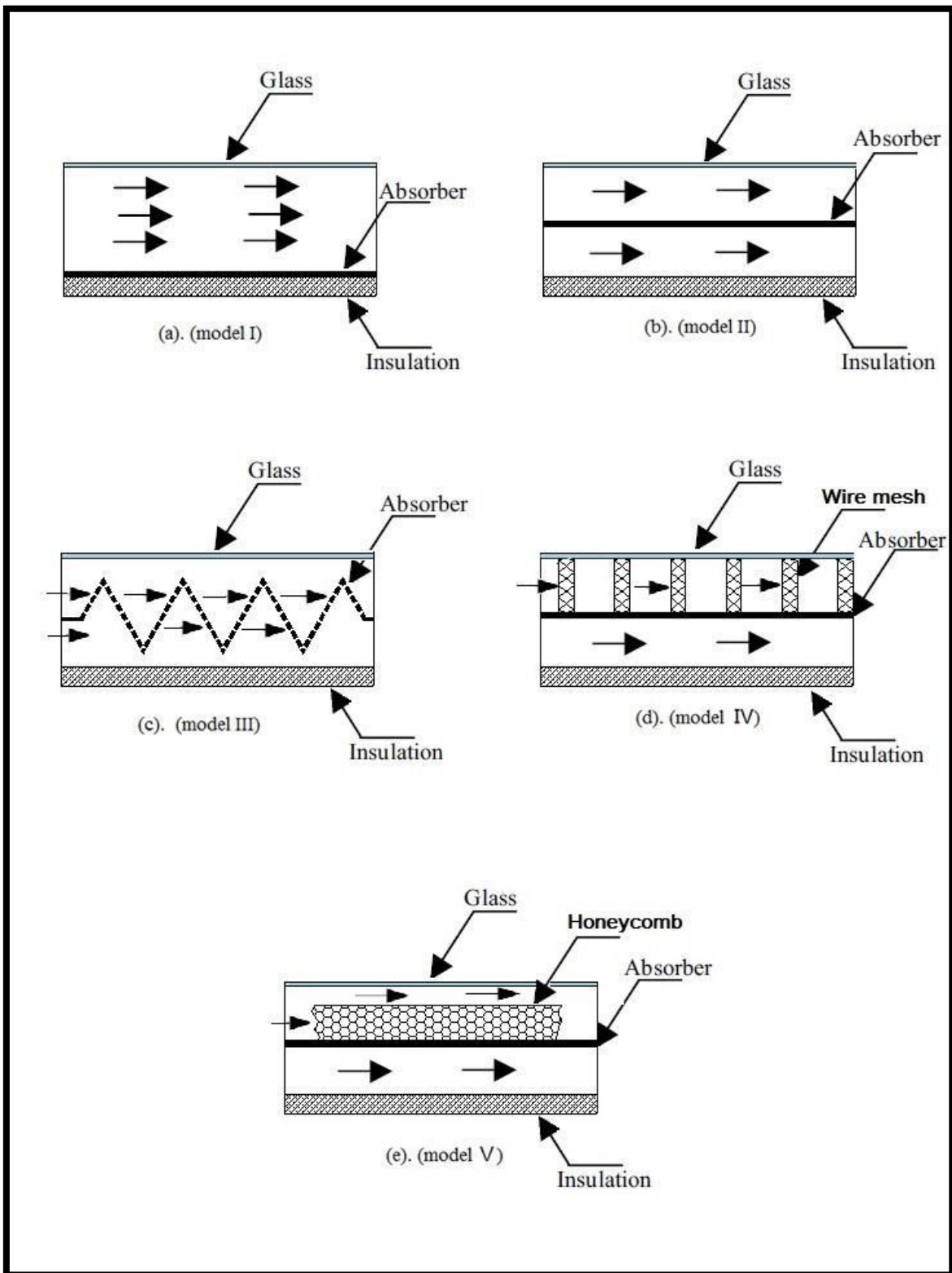
Figure 3. Schematic diagram of models of solar air collectors (I), (II), (III), (IV) and (V).
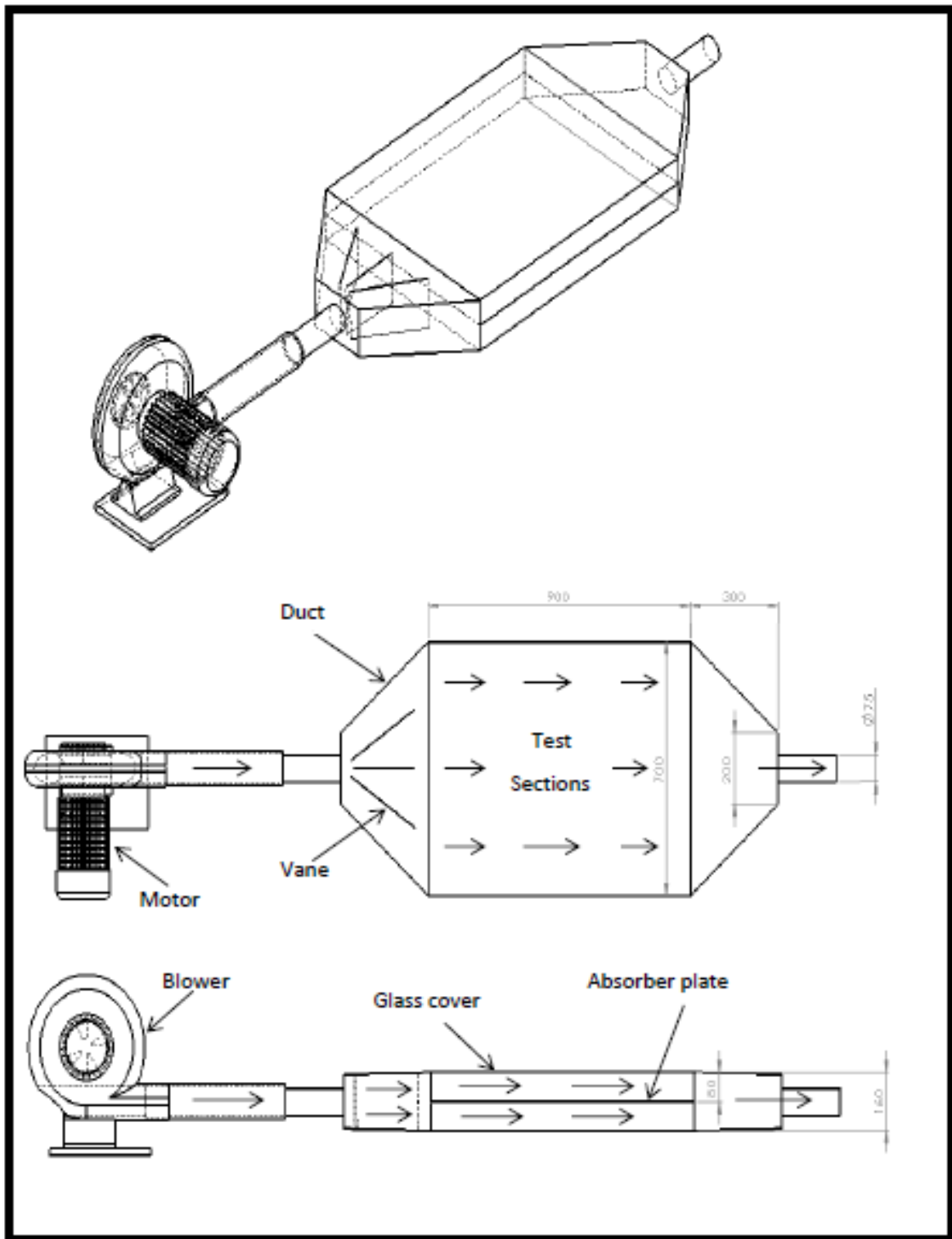
Figure 4. Schematic diagram of dual channel solar air heater (Dimensions are in mm).

Figure 5. Photographic view of dual channel (II) (right) and conventional (I) (left) SAH.

Figure 6. Photographic view of perforating "V" corrugated plate (III) (right) and conventional(I) (left) SAH.

Figure 7. Photographic view of wire mesh (IV) (right) and conventional (I) (left) SAH.

Figure 8. Photographic view of sheet of transparent honeycomb (V) (right) and conventional (I) (left) SAH.
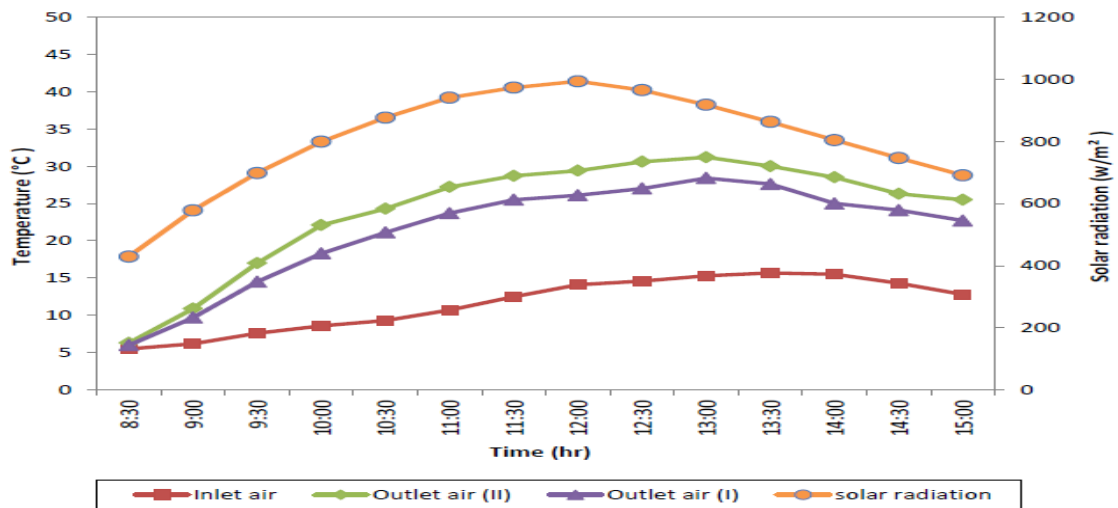
Figure 9a. Variation of air temperature with time and solar radiation for the model (II) and (I).
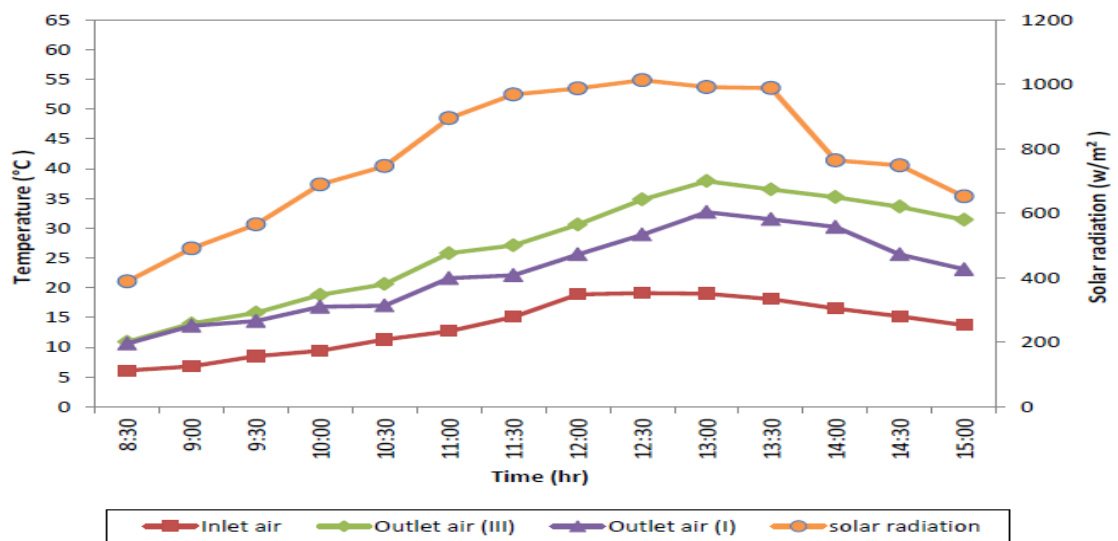
Figure 9b. Variation of air temperature with time and solar radiation for the model (III) and (I).

34
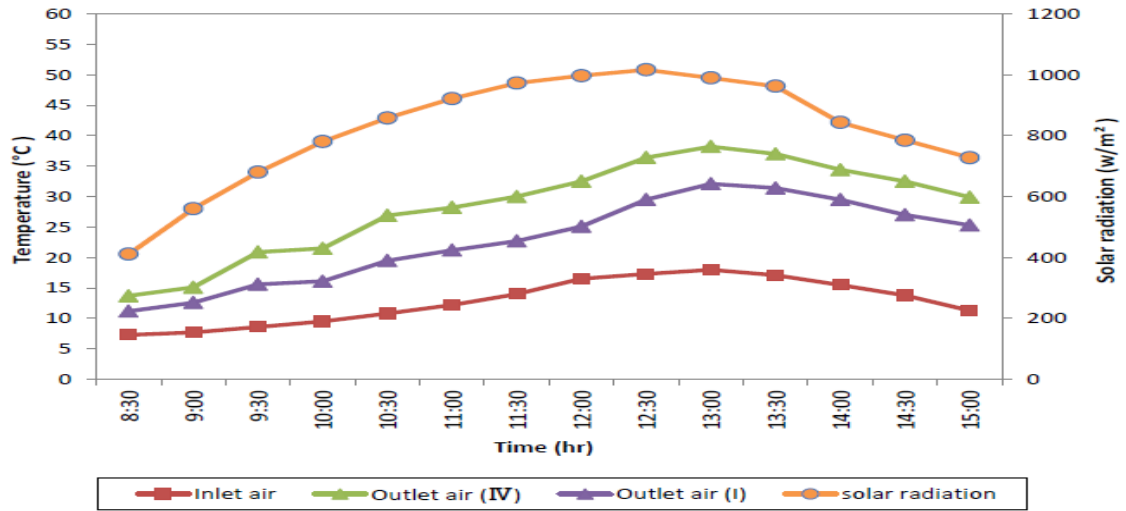
Figure 9c. Variation of air temperature with time and solar radiation for the model (IV) and (I).
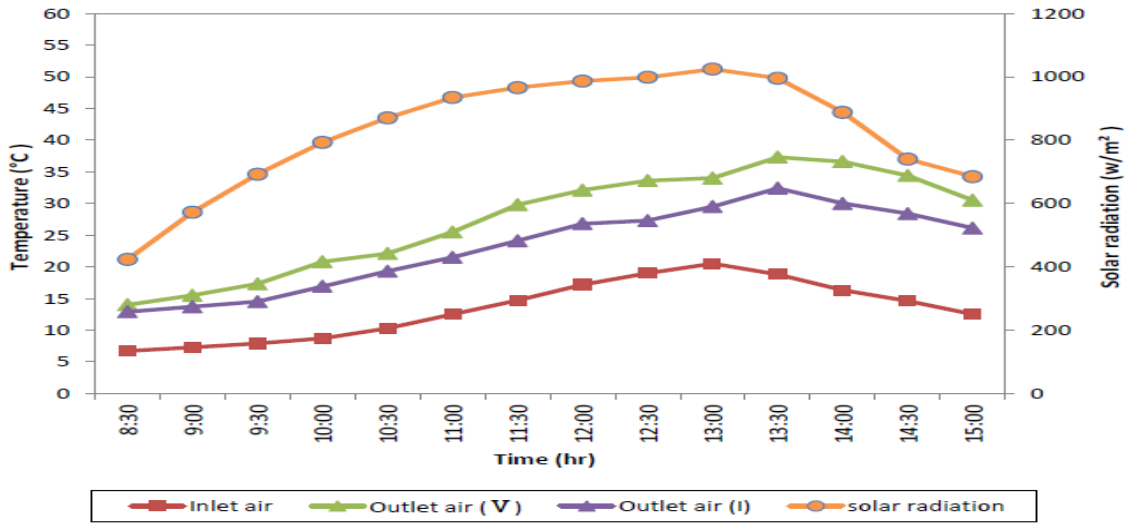
Figure 9d. Variation of air temperature with time and solar radiation for the model (V) and (I).
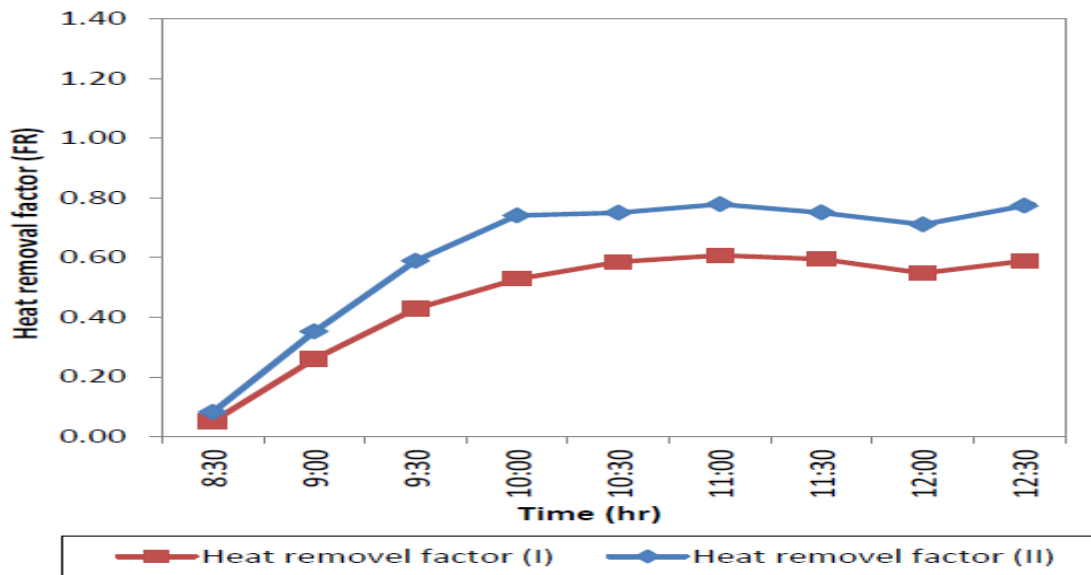
Figure 10a. Variation of heat removal factor values with time for the model (II) and model (I).

35
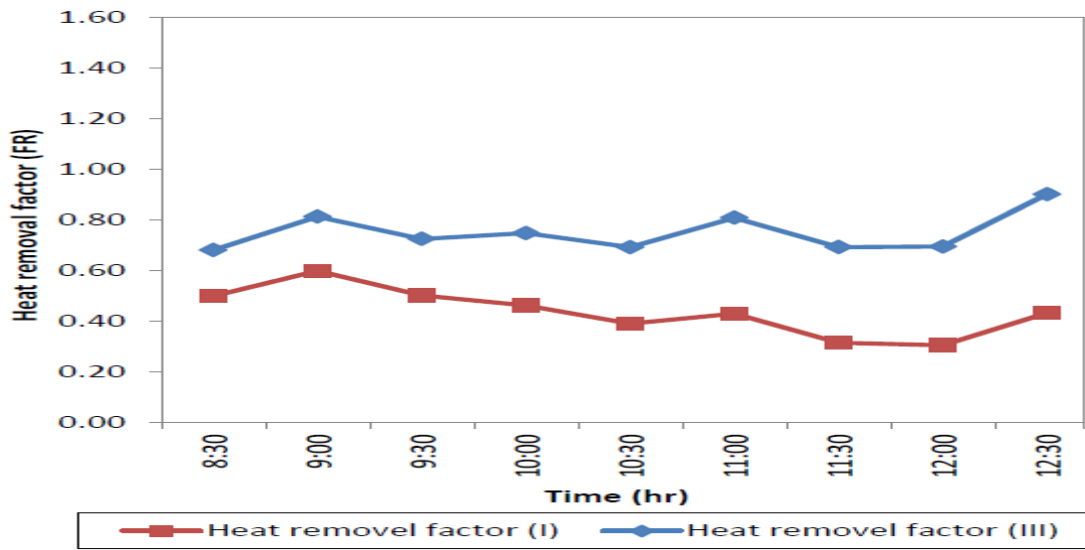
Figure 10b. Variation of heat removal factor values with time for the model (III) and model (I).
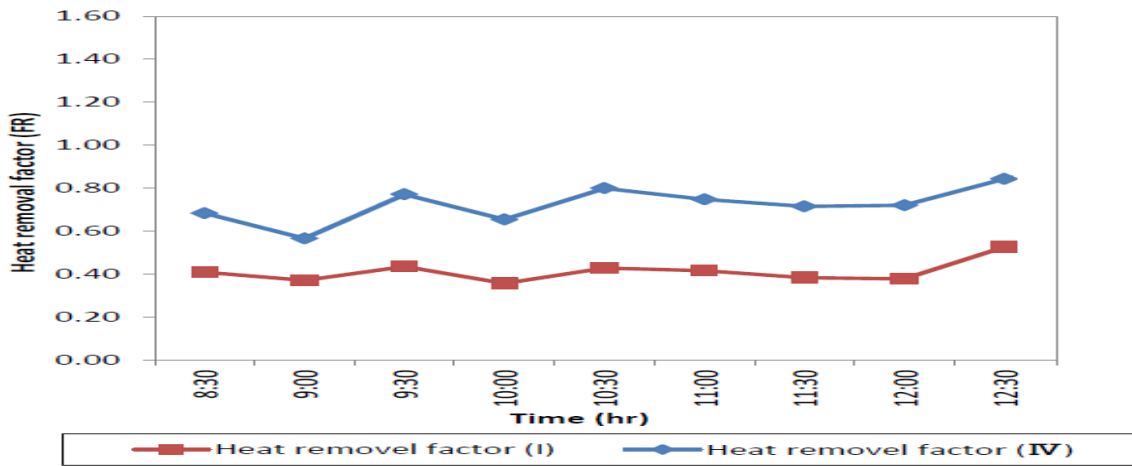
Figure 10c. Variation of heat removal factor values with time for the model (IV) and model (I).
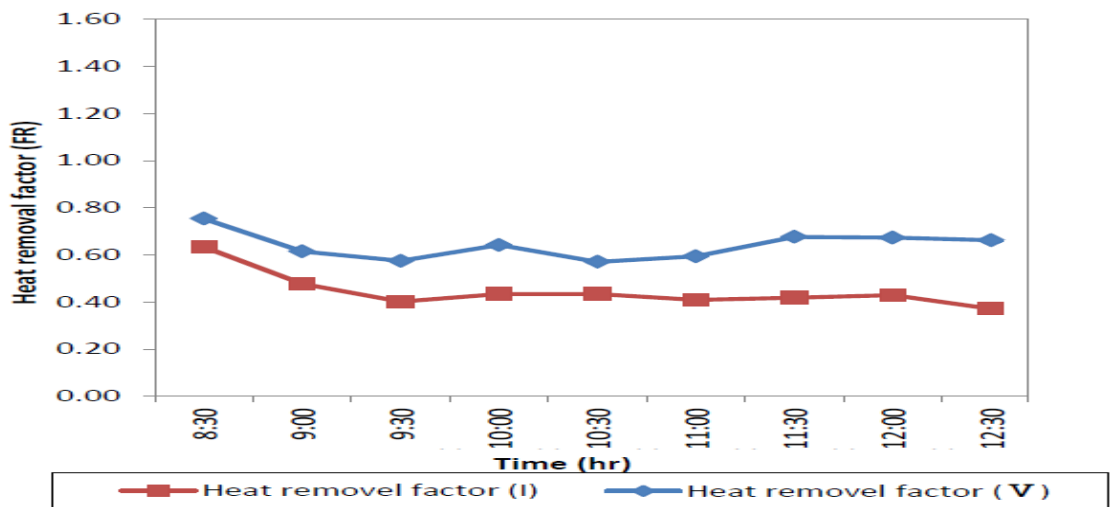
Figure 10d. Variation of heat removal factor values with time for the model (V) and model (I).
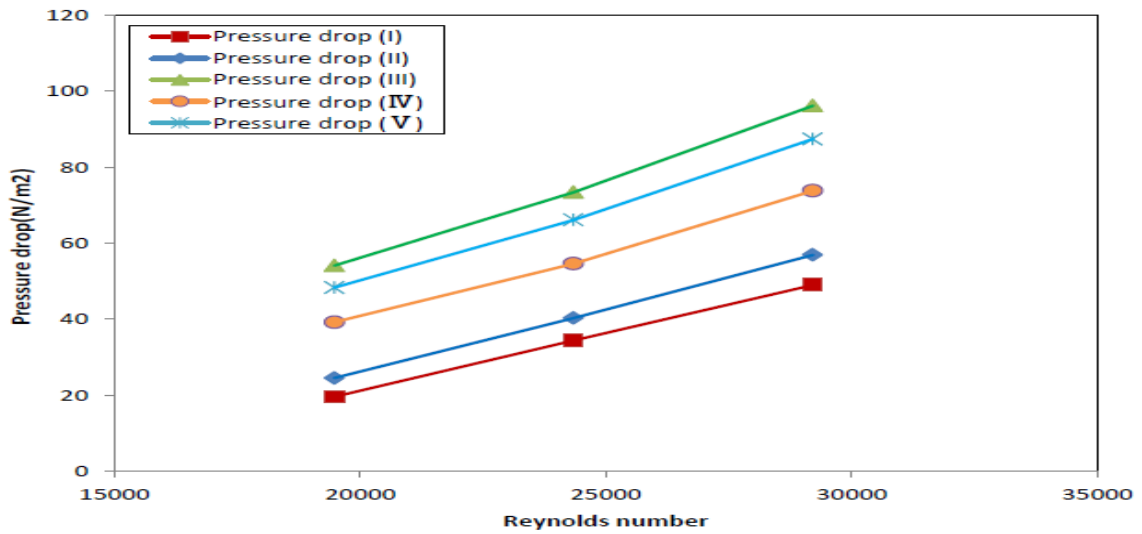
Figure 11. Variation of pressure drop with Reynold numbers for five models of solar collectors.
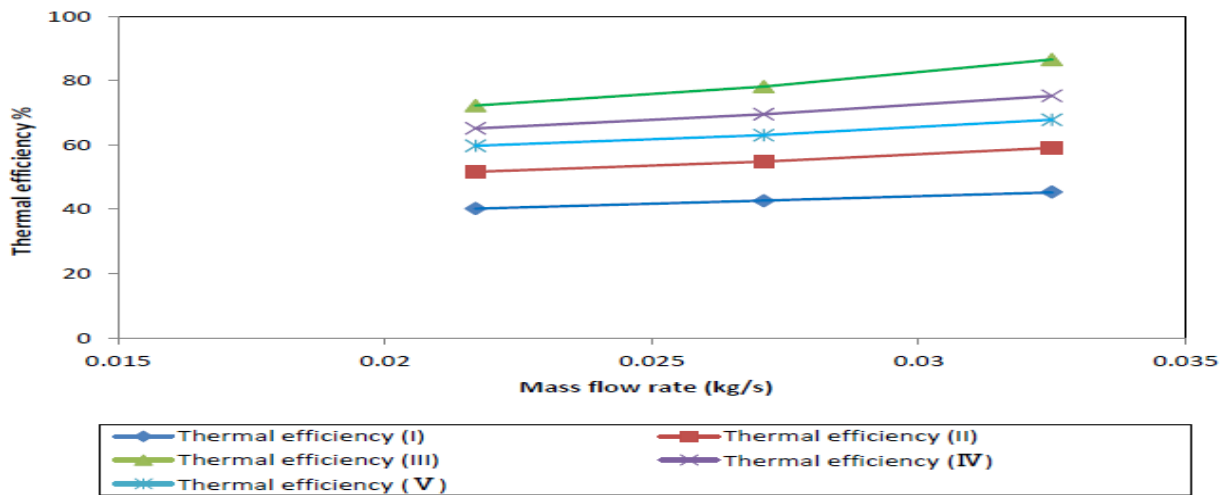
Figure 12. Variation of thermal efficiency with a mass flow rate of five models of solar collectors.
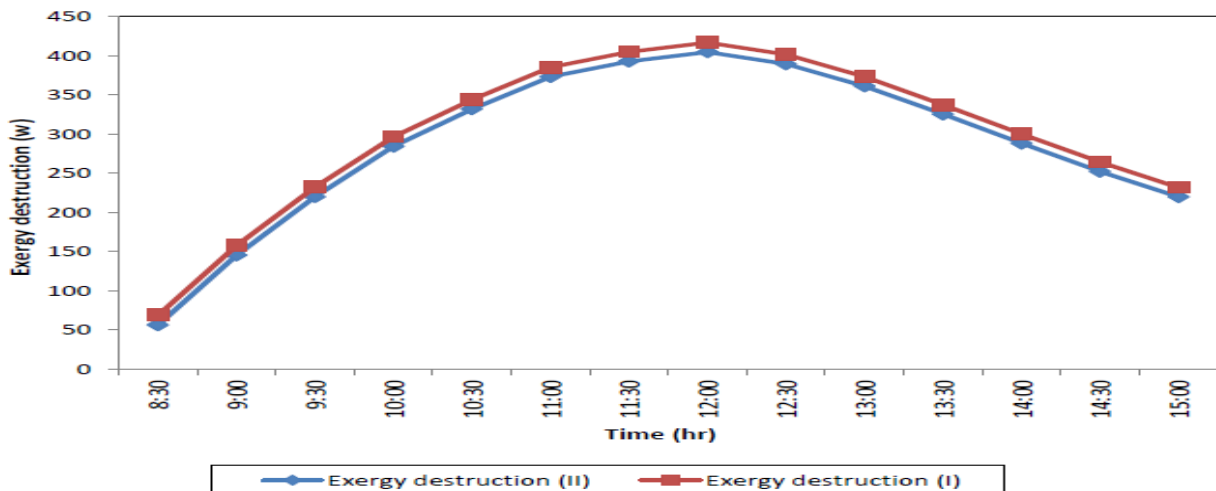
Figure 13a. Variation of exergy destruction values with time for the model (II) and model (I).

37
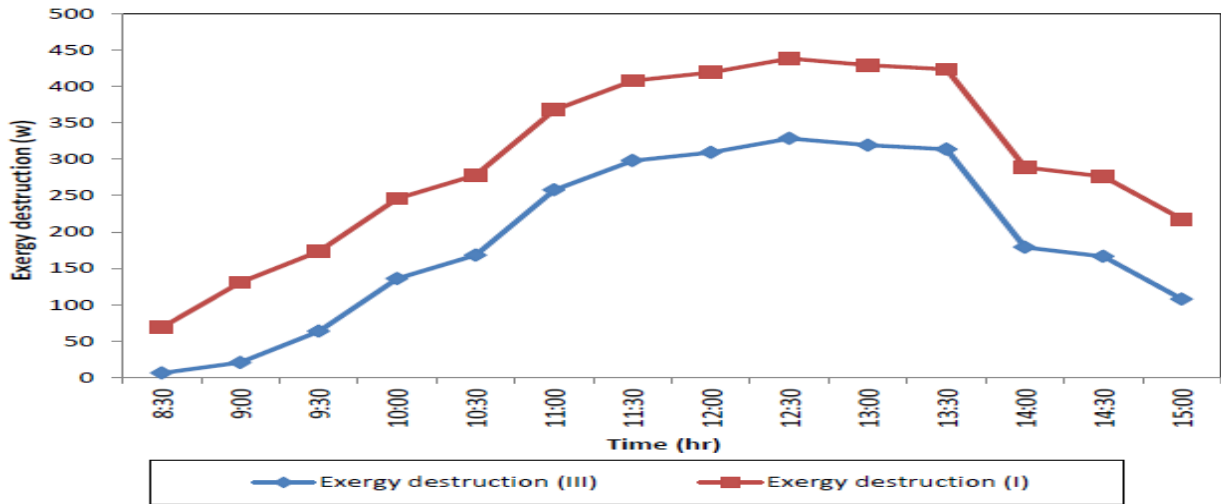
Figure 13b. Variation of exergy destruction values with time for model (III) and model (I)
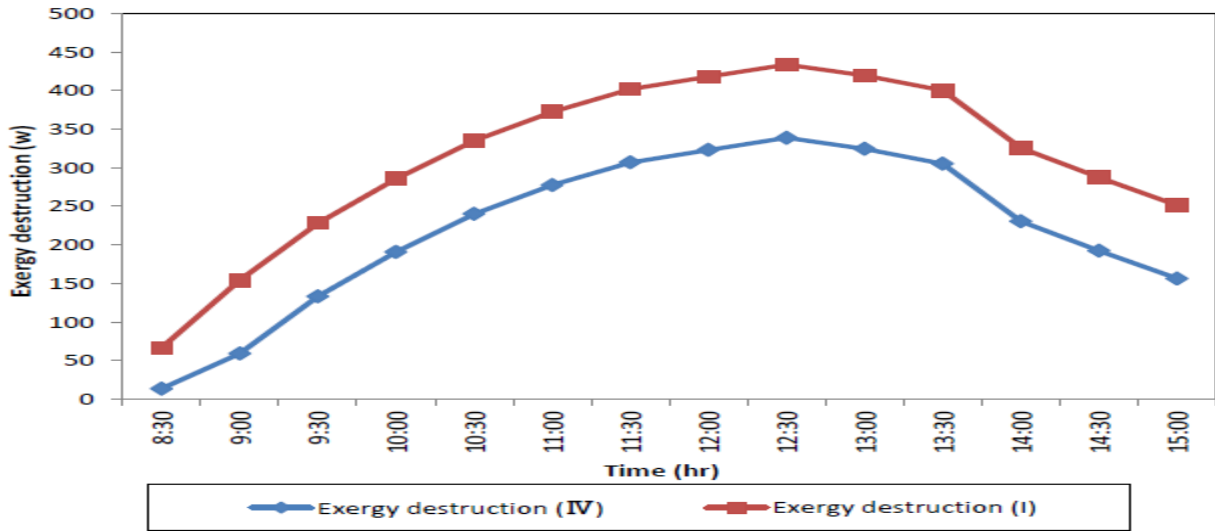
Figure 13c. Variation of exergy destruction values with time for model (IV) and model (I)
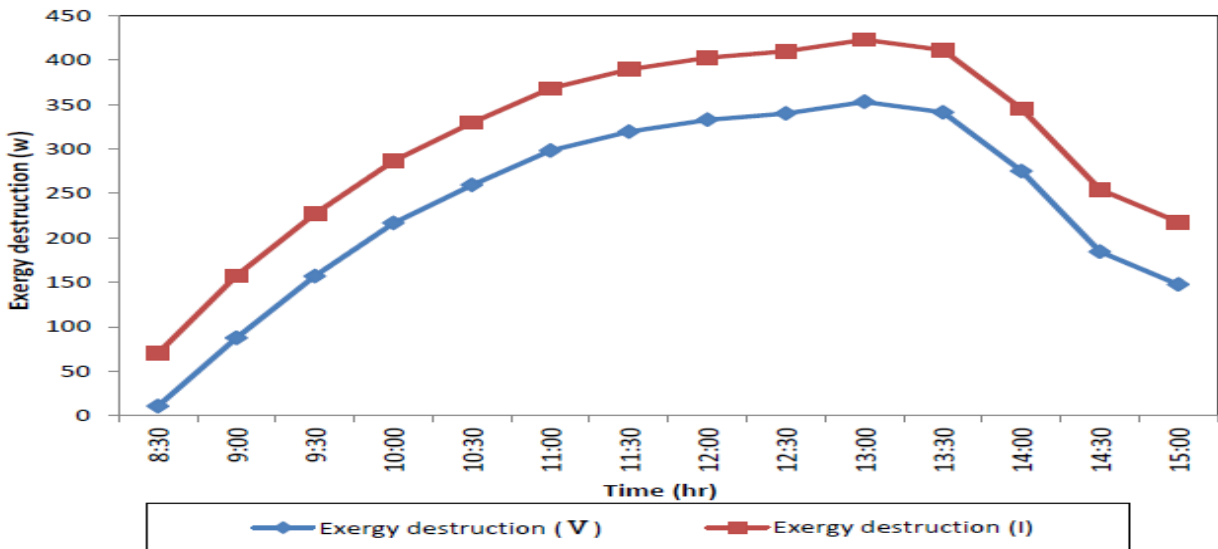
Figure 13d. Variation of exergy destruction values with time for model (V) and model (I)
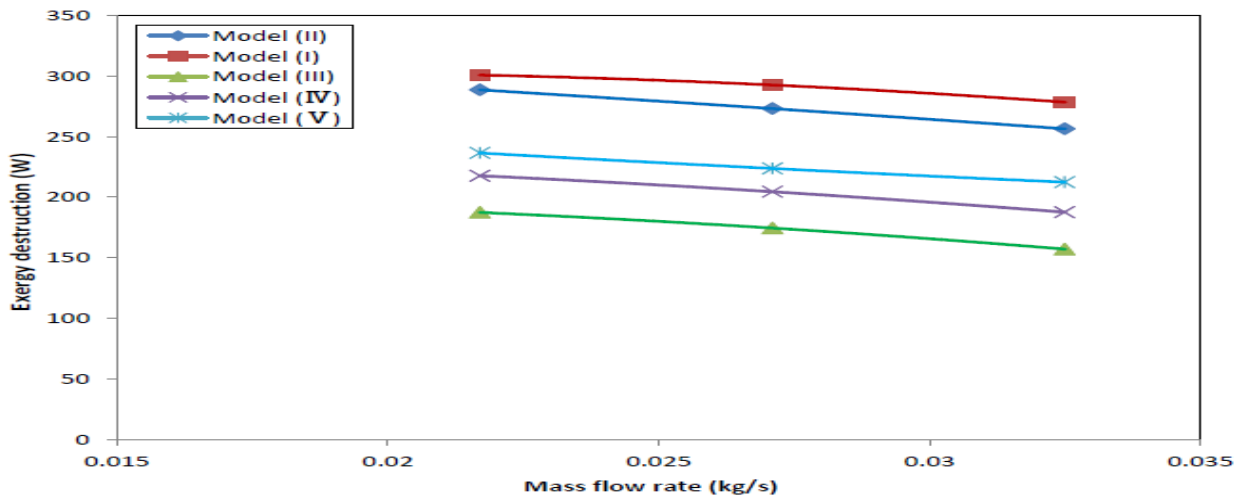
Figure 14. Variation of exergy destruction with mass flow rate for five models of solar collectors.
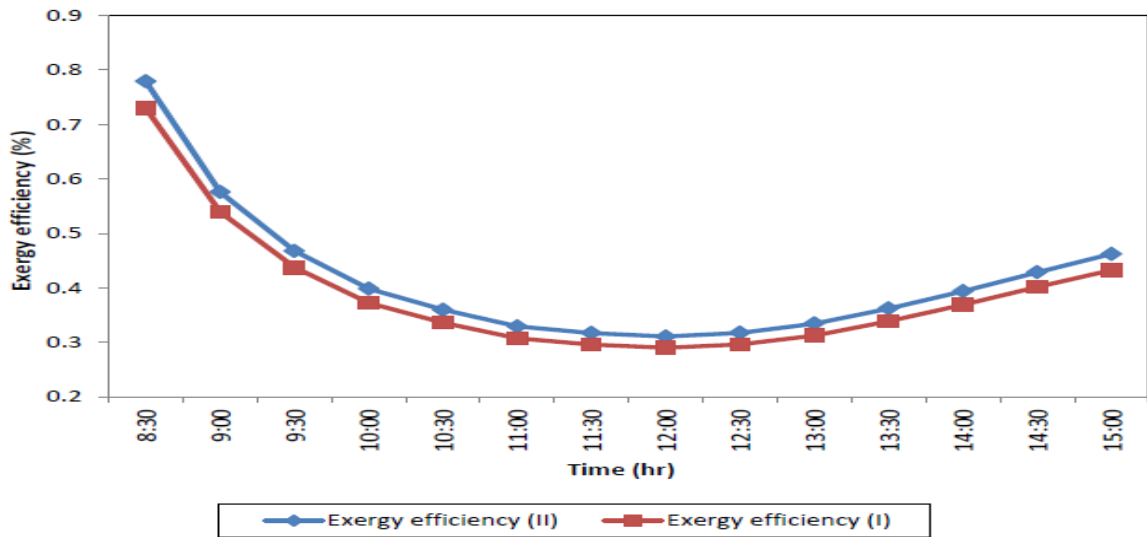
Figure 15a. Variation of exergy efficiency values with time for model (II) and model (I)
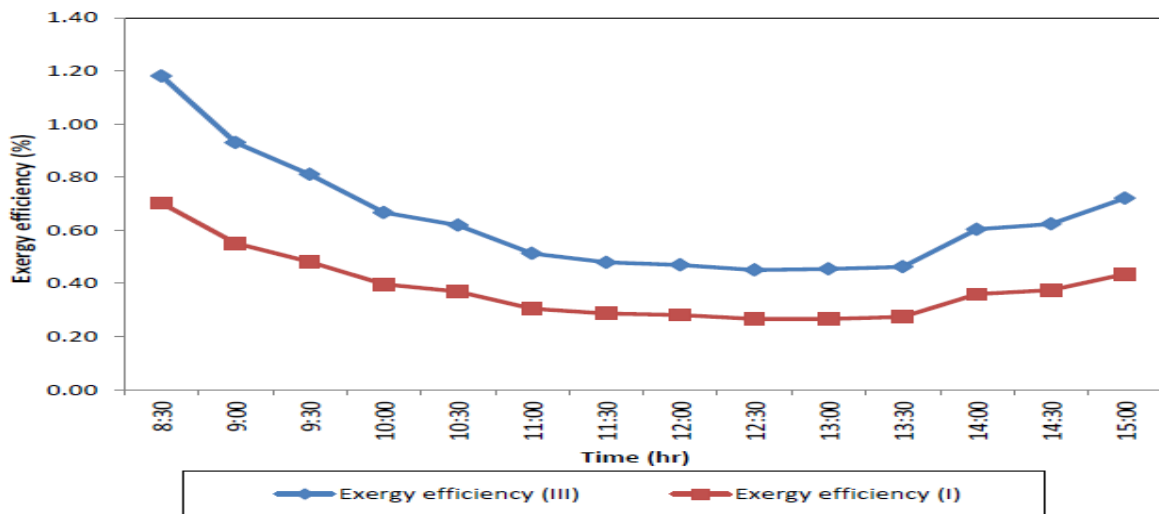
Figure 15b. Variation of exergy efficiency values with time for model (III) and model (I)
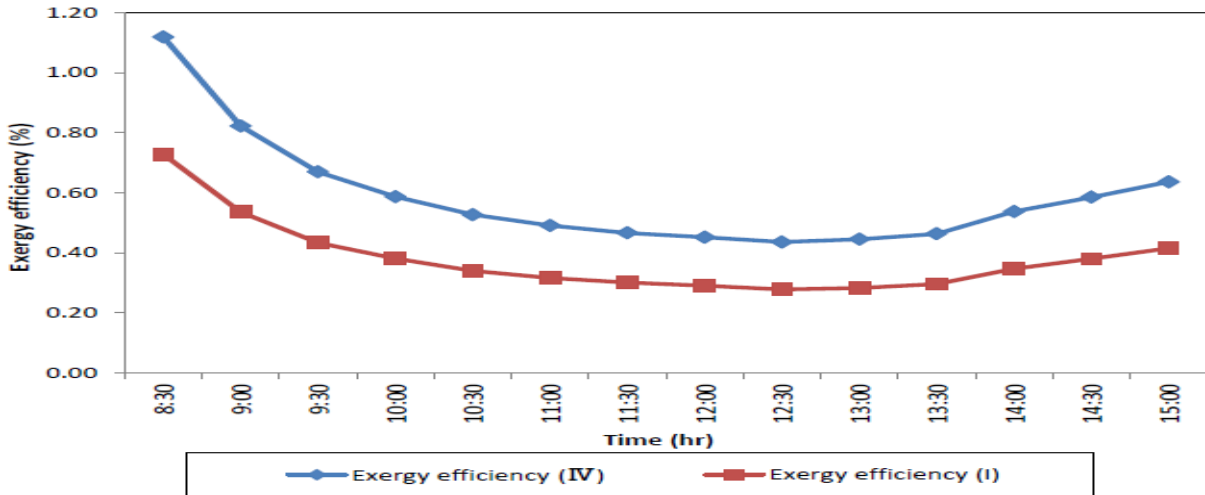
Figure 15c. Variation of exergy efficiency values with time for model (IV) and model (I)
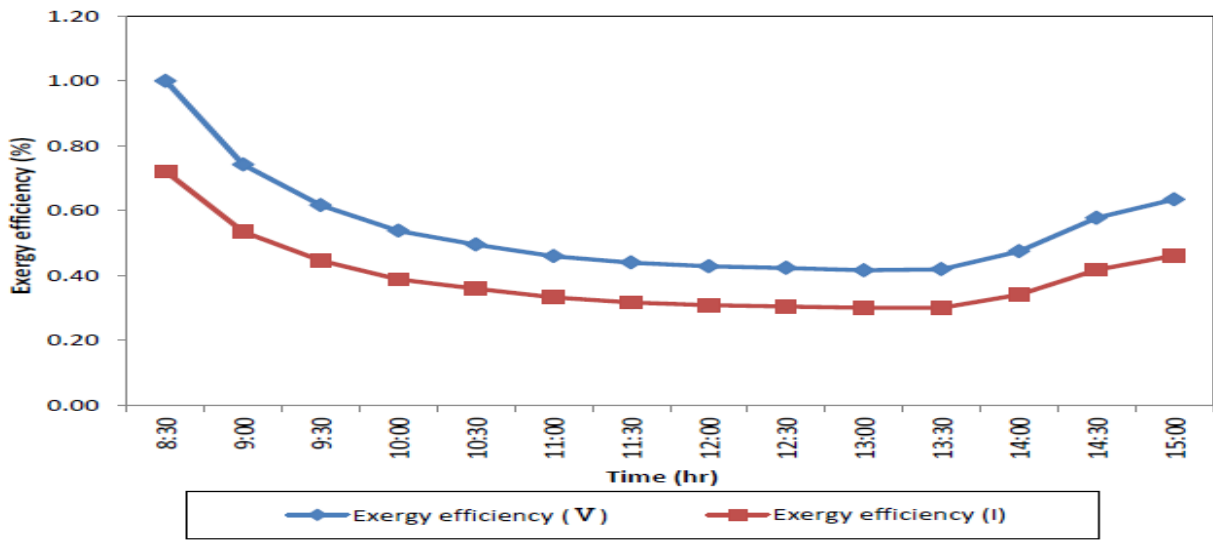
Figure 15d. Variation of exergy efficiency values with time for model (V) and model (I)
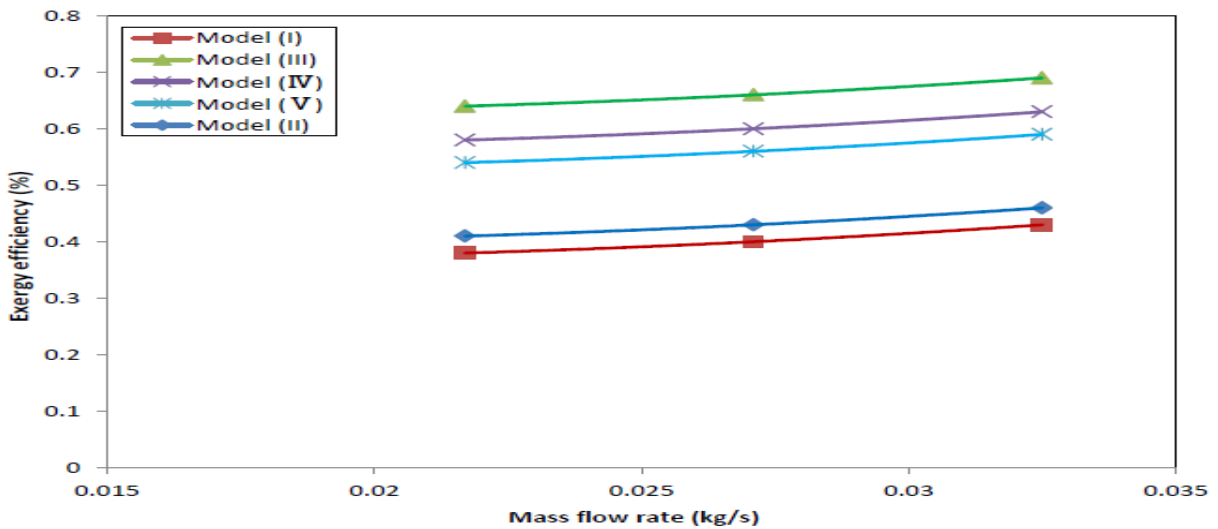
Figure 16. Variation of exergy efficiency with mass flow rate for five models of solar collectors.

40